Functional Data Analysis Assisted Cross-Domain Wi-Fi Sensing Using Few-Shot Learning

Tianya Zhao*, Ningning Wang*, Guanqun Cao†, Shiwen Mao‡, Xuyu Wang*
*Knight Foundation School of Computing and Information Sciences, Florida International University, Miami, FL 33199, USA
†Department of Statistics and Probability, Michigan State University, East Lansing, MI 48824, USA
‡Department of Electrical and Computer Engineering, Auburn University, Auburn, AL 36849, USA
Emails: tzhao010@fiu.edu, nwang012@fiu.edu, caoguanq@msu.edu, smao@ieee.org, xuywang@fiu.edu

ICC 2024 - IEEE International Conference on Communications | 978-1-7281-9054-9/24/$31.00 ©2024 IEEE | DOI: 10.1109/ICC51166.2024.10623122

***Abstract*—Recent years have witnessed rapid development of Wi-Fi sensing applications. However, the domain shift problem is still an open problem. Variations in environment, time, and detected objects can undermine the effectiveness of cross-domain sensing. This paper proposes a few-shot learning framework for Wi-Fi sensing that enables generalization to unseen domains given only a few samples. To better extract stable features, functional data analysis (FDA) is first employed as a preprocessing technique. We thoroughly evaluate our approach to different Wi-Fi sensing tasks: gesture recognition, and activity recognition. Our experimental results demonstrate that FDA assisted system improves cross-domain accuracy by 14%, 10%, and 8% on the respective tasks with five samples per class.**

***Index Terms*—Wi-Fi Sensing, Cross-Domain Sensing, Few-Shot Learning, Functional Data Analysis.**

I. Introduction

In recent years, Wi-Fi sensing has been extensively explored for diverse scenarios and applications [1]. Compared to traditional sensing approaches relying on cameras and specialized sensors, Wi-Fi sensing provides superior coverage, handles non-line-of-sight (NLOS) conditions, and reduces privacy concerns. Furthermore, Wi-Fi sensing leverages existing Wi-Fi infrastructure in homes and offices, avoiding the need for additional hardware costs. Existing Wi-Fi sensing has proven capable of detecting a diverse range of objects, from liquid detection [2] to monitoring fruit ripeness [3]. For human-centric applications, Wi-Fi sensing has enabled gesture recognition [4], activity recognition [5], breathing monitoring [6], and localization [7]. The extensive scope of Wi-Fi sensing applications underscores its potential as a versatile and promising sensing technology.

Wi-Fi signals experience propagation, reflection, refraction, and scattering before interacting with the object being measured [8]. Received signal strength indicator (RSSI) and channel state information (CSI) are commonly used to infer object actions and states. For instance, gestures impact signal propagation, leading to discernible CSI patterns. Then CSI-derived features can enable gesture recognition (GR). Deep learning-based Wi-Fi sensing employs deep neural networks (DNNs) to uncover distinct correlations between aforementioned wireless measurements and target tasks. A typical deep learning approach involves two key stages: training and inference. In the training phase, a substantial dataset is constructed, serving as the foundation for offline training of a DNN. This enables the DNN to learn accurate mapping relationships. In the inference stage, the trained model is deployed to make predictions about incoming inputs.

While deep learning-based wireless sensing techniques have demonstrated their efficacy, domain shift remains an open challenge. Wireless signals inherently contain substantial information specific to the environment and the subject, owing to the multipath propagation characteristics of radio signals that depend on factors like the environment, objects involved, and the nature of the sensing task. Performing the same sensing task under different temporal, spatial, or object-related conditions may introduce variations in signal propagation. These task-agnostic parameters collectively define a domain. In general, the source domain refers to the domain during the training phase, while the target domain refers to the domain during the inference phase. When the target domain differs from the source domain (e.g., different environments), domain shifting occurs and can potentially lead to a reduction in Wi-Fi sensing accuracy.

Therefore, addressing the domain shift problem is imperative to ensure the dependable deployment of wireless sensing systems. For traditional supervised learning DNNs, one approach to addressing this challenge involves retraining the model using a new dataset containing the target domain. However, this retraining process demands a substantial volume of target domain data and is time-consuming, making it impractical to implement. Current solutions primarily concentrate on adversarial domain adaptation (ADA) [9]–[11] and few-shot learning [12]–[15]. The adversarial domain adaptation-based method also requires expansive multi-domain training data and a relatively complex training process, which can be cumbersome to deploy. *While various deep learning techniques have been proposed to mitigate the domain shift problem, there has been limited exploration of how to process the input data itself to enhance robustness to domain shifts.* Traditional methods typically consider various filters (e.g., Hampel Filter) and transforms (e.g., Fast Fourier Transform) to process data [1], which can remove outliers and obtain additional frequency information. However, these methods may not reveal the underlying data characteristics.

In this paper, we incorporate statistical methods to uncover

signal properties and mitigate domain shift issues. Specifically, we employ functional data analysis (FDA) to extract domain-invariant features by denoising, reducing latent domain effects, and revealing input data's functional characteristics. Then, we opt for few-shot learning (FSL) to enable predictions based on feature similarity to address the domain shift problem. Meanwhile, FSL enables models to generalize from limited target domain data as a meta-learning approach. This is well-suited for wireless systems. For instance, a dual-path base network with metric-based meta-learning improves adaptability without requiring a large amount of target domain data and cumbersome retraining in [12]. Nevertheless, previous FSL-based methods mainly focus on human activity recognition (HAR) tasks. Our paper further broadens the problem scope, making it effective for various sensing tasks including HAR and GR. The major contributions made in this paper are summarized as follows.

- To the best of our knowledge, this is the first work to employ functional data analysis to help mitigate domain shift issues in Wi-Fi sensing.
- We propose a unified few-shot learning framework applicable to various Wi-Fi sensing tasks, enabling adaptability to new domains given only a few samples.
- We experimentally demonstrate that our proposed method can significantly increase both source and target domain accuracy across different Wi-Fi sensing applications.

The remainder of this paper is organized as follows. Section II introduces the background and motivation of our work. In Section III, we introduce our system design. Experimental results are presented in Section IV. We conclude this paper in Section V.

II. Background and Motivation

A. Wi-Fi Sensing

Recent Wi-Fi sensing systems widely use CSI to achieve fine-grained sensing. CSI is impacted by multi-path effects and represents the Channel Frequency Response (CFR) as

$$H(f,t) = \sum_{l=0}^{L} \alpha_l(t) e^{-j2\pi f \tau_l(t)}, \tag{1}$$

where L is the number of propagation paths, $\alpha_l(t)$ and $\tau_l(t)$ represent the signal attenuation and propagation delay along path l, respectively, and f is the carrier frequency [8]. CSI encapsulates various channel properties of wireless signals, accounting for factors like scattering, environmental attenuation, and distance attenuation. Therefore, human motion along the signal propagation path produces distinguishable CSI patterns, enabling Wi-Fi sensing. The sensitivity of CSI to signal propagation changes is the fundamental principle behind Wi-Fi sensing techniques. In this paper, we consider Wi-Fi sensing with CSI amplitude due to its stability [1], [7].

B. Functional Data Analysis

FDA analyzes data that can be represented as functions over a continuous variable. Functional data is inherently high-dimensional or infinite-dimensional, with the basic unit being a function rather than a single data point [16]. To utilize the continuity of functional data and find a more useful finite representation, FDA techniques often decompose functional inputs into a set of basis functions as [17]:

$$X(t) \approx \sum_{j=1}^{J} \alpha_j \phi_j(t), \tag{2}$$

where $\{\phi_j(t)\}_{j=1}^{J}$ is a set of J continuous basis functions and $\{\alpha_j\}_{j=1}^{J}$ denotes the corresponding coefficients. One strength of FDA is that it can easily accommodate measurement errors [18]. This makes it a useful tool for denoising and unveiling the properties of wireless signals.

C. Few-Shot Learning

FSL is a type of meta-learning where models aim to emulate human-like learning [19]. These models gain knowledge from known tasks, which they can then apply to new tasks with only a small number of labeled examples. In this paper, known tasks refer to sensing tasks from source domains, while new tasks come from target domains. The rationale is straightforward: by learning the similarities and differences present in source domain data, FSL models can make predictions on new target tasks by comparing their similarities with a minimal amount of labeled target data. Unlike traditional supervised learning, FSL adopts a different approach to partitioning datasets. The dataset $\mathcal{D}$ in each domain is divided into a support set $\mathcal{D}_s$ for learning and a query set $\mathcal{D}_q$ for training and testing. A common FSL paradigm is the N-way K-shot scheme, where N denotes the number of classes used for training from the support set and K refers to the number of labeled examples per class.

D. Motivation

While deep learning has achieved excellent performance for wireless sensing tasks, these models struggle when faced with new environments or objects not seen during training. Moreover, collecting and labeling large wireless datasets for each new domain is challenging and often infeasible. To address this, FSL offers a solution by enabling models to make predictions using just a small amount of new data. However, directly applying FSL to wireless input may not work well, as wireless signals are impacted by many factors during propagation that can differ across domains.

As depicted in Fig. 1a, source domain data and target domain data have different distributions. To extract more generalizable features for classification, we first process the raw input data using FDA, which is a statistical technique to remove measurement errors and reveal functional features. Fig. 1b illustrates the T-SNE result for FDA-processed data. The distance between different clusters is increased, while clusters themselves are tighter. This helps FSL better resolve domain shift issues. FDA serves to attenuate the effects of domain-specific propagation factors, allowing the FSL model to focus on more generalizable features. By combining FDA as a preprocessing step with FSL, we can rapidly adapt DNNs

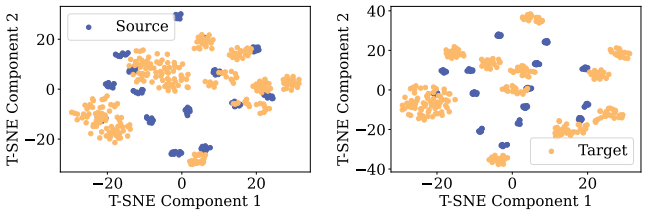

(a) Original data in the source domain and target domain. (b) FDA processed data in different domains.

Fig. 1: T-SNE visualization of 15 activities.

to new wireless sensing tasks and environments using only a few labeled examples, without a costly retraining process.

III. System Design

This section outlines the cross-domain wireless sensing system design, which contains three key modules as shown in Fig. 2: (i) dataset construction, (ii) the data preprocessing module, and (iii) the FSL training and testing module. We first formulate the cross-domain few-shot learning problem for wireless sensing. We then elaborate on how these modules are integrated into a wireless system that leverages FSL to enable rapid adaptation to unseen domains with limited labeled data.

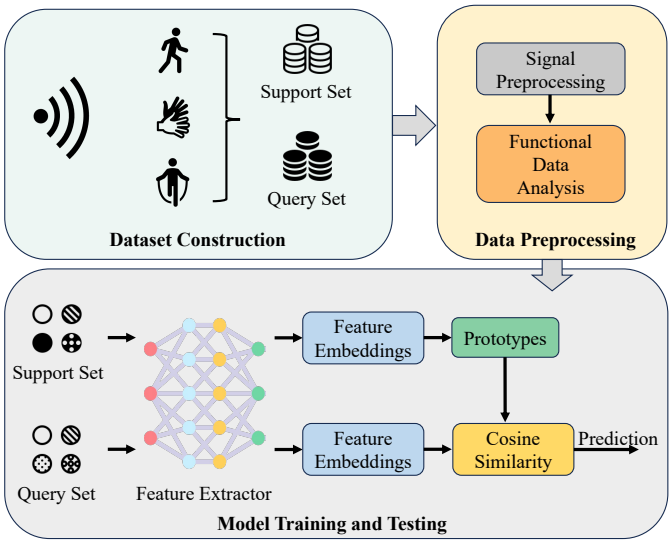

Fig. 2: System overview.

A. Problem Formulation

The objective of this study is to achieve rapid adaptation to any new target domain with minimal labeled data. To evaluate the effectiveness of the proposed cross-domain sensing system, we evaluate it on two different sensing tasks: HAR and GR. In these two sensing tasks, a three-dimensional CSI tensor $\mathbf{x} \in \mathbb{R}^{p \times s \times a}$ is generated for sensing, where p denotes the number of packets, s refers to subcarrier groups, and a is transmitter-receiver antenna pairs. To equip our system with a feature extractor f_θ possessing strong generalization capabilities, we customize prototypical networks (PTN) [20], which is a metric-based FSL approach.

The overall learning process is structured as follows. We first train the feature extractor f_θ using source domain datasets. In the target domain, we randomly select K samples for each class to form support set $\mathcal{D}_s = \{\mathbf{x}_s, y_s\}^{K \times N}$ and K_q samples per class as query set $\mathcal{D}_q = \{\mathbf{x}_q, y_q\}^{K_q \times N}$ in each episode. In this work, the number of classes N remains the same, but the samples differ between the support set and the query set, specifically, $\mathcal{D}_s \cap \mathcal{D}_q = \varnothing$. The overall objective function can be expressed as below:

$$\theta^* = \arg\max_\theta \mathbb{E}_\mathcal{D} \left[\sum_{\mathcal{D}_s} \sum_{\mathcal{D}_q} m\left(f_\theta(\mathbf{x}_q).f_\theta(\mathbf{x}_s), y_s\right) \right], \quad (3)$$

where $m(\cdot)$ is our metric-based FSL framework. This objective function necessitates that the features extracted from both the support set and the query set exhibit high similarity. After acquiring an effective feature extractor f_θ, it can be deployed to unseen domains to produce domain-independent features from the same class.

B. Data Preprocessing

In this module, CSI amplitudes are preprocessed before being fed to the feature extractor. First, we normalize $\mathbf{x}$ by $\frac{\mathbf{x}-min(\mathbf{x})}{max(\mathbf{x})-min(\mathbf{x})}$ along the time/packets dimension. The primary objective of this normalization process is to attenuate the impact of the magnitude of values, thereby concentrating more on the CSI patterns.

Subsequently, FDA is applied to further eliminate measurement errors and uncover the underlying information. As described in Section II-B, functional data can be represented by a set of basis functions. Given the inherent relationship between wireless signals and the Fourier transform, we choose to employ the Fourier basis as the basis functions:

$$\phi_0(t) = \frac{1}{\sqrt{2}}, \quad (4)$$

$$\phi_{2j}(t) = \frac{cos(\frac{2\pi j}{T}t)}{\sqrt{\frac{T}{2}}}, \ \phi_{2j-1}(t) = \frac{sin(\frac{2\pi j}{T}t)}{\sqrt{\frac{T}{2}}}, \quad (5)$$

where T denotes the period. In this paper, FDA processes CSI tensors $\mathbf{x}$ along the time dimension using the same Fourier basis functions.

Fig. 3a shows the first five elements of the Fourier basis functions. The choice of the number of basis functions can significantly impact the representation of the signal. Fig. 3b illustrates the CSI data for a single subcarrier and transmitter-receiver pair. Fig. 3c presents the CSI data after FDA processing with 141 Fourier basis functions, while Fig. 3d depicts the CSI data processed by only 41 Fourier basis functions. Using a larger number of basis functions tends to make the data curve closely resemble the original data. On the other hand, employing fewer basis functions results in a data pattern that primarily captures the fundamental characteristics, creating a smoother representation, albeit with some potential deviation from the original curves.

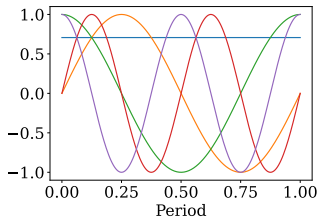

(a) The example of first 5 Fourier basis elements.

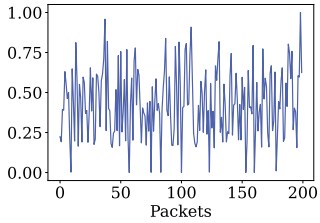

(b) Original CSI example on the packet dimension.

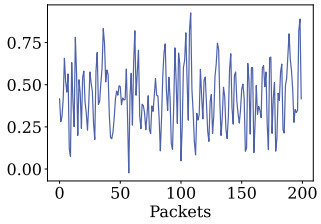

(c) Representation on a larger basis $J = 141$.

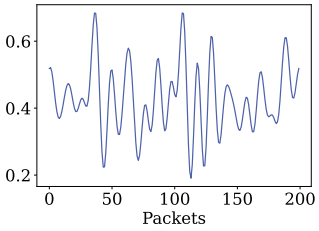

(d) Representation on a smaller basis $J = 41$.

Fig. 3: Original data and FDA processed data.

C. Cross-Domain Sensing

In this module, we modify the PTN to extract domain-independent features from FDA-processed CSI tensors to improve cross-domain sensing accuracy. Convolutional neural networks (CNNs) have demonstrated their proficiency in extracting meaningful features from input data. This makes CNNs a well-suited feature extractor for Wi-Fi sensing tasks. In this paper, we deploy a simple CNN model that closely resembles the architecture presented in [4]. The key difference lies in the final linear layer, which generates a 256-dimensional vector employed as the feature embedding. To standardize embedding scales and further improve classification accuracy, we restrict the embedding vectors to reside on a hypersphere within the same radius. Therefore, an L_2-norm layer is added after the final linear layer as below:

$$f_\theta(\mathbf{x}) = \frac{f'_\theta(\mathbf{x})}{\|f'_\theta(\mathbf{x})\|_2}, \tag{6}$$

where $f'_\theta(\mathbf{x})$ represents the original output embedding before the L_2-norm $\|\cdot\|_2$, and $f_\theta(\mathbf{x})$ denotes the final normalized feature embeddings.

During the training phase, the feature extractor is trained using source domain data. Since the label space remains consistent in the same sensing task, and only the input space is influenced by various domains, we can fully exploit the relationship between feature embeddings and corresponding labels by adding a linear probe C_ϕ after the feature extractor. The output size of C_ϕ is adjusted based on the number of target classes. Cross entropy function can be used to calculate the loss to guide parameter updates of the feature extractor and linear probe as follows:

$$\mathcal{L} = -\sum_i y_i \cdot log(C_\phi(f_\theta(\mathbf{x}_i))). \tag{7}$$

In the inference stage, the linear probe is discarded. The feature extractor is deployed to extract feature embeddings and generate stable prototypes. For the support set $\mathcal{D}_s$, each input is fed to the feature extractor to generate a feature embedding. Then, prototypes are generated by taking the average of the embedding vectors from the same class as follows:

$$\mathbf{c_n} = \frac{1}{K} \sum_{\mathbf{x}_i \in \mathcal{D}_s} f_\theta(\mathbf{x}_i),\ n = (1, 2, \cdots, N), \tag{8}$$

where $\mathbf{c_n}$ denotes the prototype of class n. By incorporating the information from the K samples to generate the prototype, the effect of the domain is minimized.

After the prototypes have been generated, query data $\mathcal{D}_q$ can be classified by comparing the similarities between query embeddings and prototypes in the embedding space as

$$P(y_q = n'|\mathbf{x}_q) = \frac{exp(s(f_\theta(\mathbf{x}_q), \mathbf{c_{n'}}))}{\sum_n exp(s(f_\theta(\mathbf{x}_q), \mathbf{c_n}))}, \tag{9}$$

where s is the similarity function defined as

$$s(f_\theta(\mathbf{x}_q), \mathbf{c_{n'}}) = \frac{f_\theta(\mathbf{x}_q) \cdot \mathbf{c_{n'}}}{\|f_\theta(\mathbf{x}_q)\|_2 \|\mathbf{c_{n'}}\|_2}. \tag{10}$$

The greater similarity value indicates a higher likelihood that the input query data belongs to the class associated with the corresponding prototype.

IV. Experiment Study

A. Datasets and Experimental Setup

In all experiments, the learning rate was set to 0.0001. K, K_q, and max epochs were set to 5, 20, 50, respectively. The value of N was set to the total number of classes. The shape of the input CSI tensor was set to $200 \times 30 \times 3$. All experiments were conducted on a server with an Intel Xeon E5-2650L v4 CPU and 8 NVIDIA GeForce GTX 1080Ti GPU.

We comprehensively discuss our proposed system on three public datasets as shown in Table. I.

TABLE I: Dataset Summary.

	Task	Domain Partition	# domains	# classes
SignFi	GR	Environment	2	276
Wiar	HAR	User	9	16
Widar	HAR	Environment + User	3	6

1) SignFi: The SignFi dataset [4] encompasses a diverse set of 276 sign language gestures. The domains are divided based on the environment. The lab environment data is used as the source domain, while the home environment data is used as the target domain.

2) Wiar: The Wiar dataset [21] comprises 16 distinct human activities that encompass movements of the torso, arms, and hands. For this work, data from 6 users is utilized as the source domain data, while data from 3 other users serves as the target domain data.

3) Widar: The Widar dataset [22] is expansive in scale, so only subsets are used. Specifically, 6 different activities performed by three different users in two different rooms are selected. The combination of different rooms and users creates distinct target domains.

B. Evaluation on Cross-domain Sensing

To demonstrate the effectiveness of our proposed method in addressing domain shift issues, we evaluate several classic methods in this section. Specifically, we assess the performance of traditional methods such as K-Nearest Neighbors (KNN) and CNN. As discussed in Section I, ADA and FSL are two promising techniques for solving domain shift problems. Therefore, we also examine the performance of the ADA method deployed in [9] and the FSL approach without FDA preprocessing. To ensure a fair comparison, the CNN and the feature extractor architecture of ADA method are identical to the feature extractor used in our approach. The overall results are presented in Table. II.

TABLE II: Target domain accuracy.

	KNN	CNN	ADA	FSL	**Ours**
SignFi	0.0018	0.0029	0.2276	0.7938	0.9332
Wiar	0.0714	0.0643	0.6727	0.6625	0.7625
Widar	0.3385	0.3139	0.4100	0.6073	0.6833

For both HAR and GR tasks, traditional methods completely fail to achieve strong performance when evaluated on the unseen target domain. Widar appears to have higher accuracy than the other two datasets due to the fact that Widar only needs to distinguish fewer categories compared to the other datasets. Compared to conventional models, both ADA and FSL can significantly boost cross-domain sensing accuracy across three cases. In particular, FSL generally outperforms ADA, likely because FSL models can incorporate some target domain information and extract more meaningful features. In all cases, ADA only slightly outperforms FSL on Wiar, which may be due to the use of more data from different domains in the training phase.

Our proposed FDA-assisted FSL approach further enhances cross-domain sensing performance across all scenarios. The most substantial improvement is observed in SignFi, which improves by about 70% and 14% than ADA and FSL, respectively. For the HAR cases, our method increases approximately 10% and 8% over the FSL approach. For the Widar dataset, while our method achieves an accuracy of approximately 68% in unseen target domains, it continues to outperform other approaches. The relatively lower performance in this case may be attributed to the increased complexity of source and target domains, which are influenced by the greater diversity in torso positions, body orientations, and Wi-Fi receiver locations.

C. Evaluation on FDA

In general, employing FDA as a data preprocessing technique helps improve both source domain and target domain accuracy. The selection of FDA basis functions impacts performance across different sensing tasks, as demonstrated in Fig. 4 and Fig. 5. For Wiar, the B-spline basis leads to lower accuracy, while the Fourier basis boosts it. Across these Wi-Fi sensing tasks, using Fourier basis functions leads to better performance compared to B-Spline bases. This is reasonable

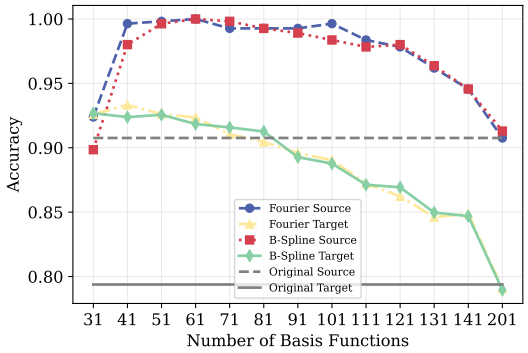

Fig. 4: The classification accuracy on SignFi for different numbers of basis functions with various bases.

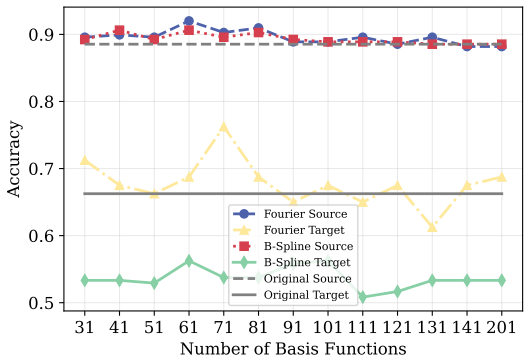

Fig. 5: The classification accuracy on Wiar for different numbers of basis functions with various bases.

since wireless signals are intrinsically related to the Fourier transform. Therefore, the set of Fourier basis functions may capture more meaningful information about the wireless data.

In addition, the number of basis functions also affects the cross-domain sensing performance. As discussed in Section III-B, more basis functions can describe finer data details, while fewer basis functions aim to smooth the data and capture significant characteristics. As a result, when the number of basis functions is set to 201, the performance of our method is similar to the original FSL without FDA processing. This suggests that an excessive number of basis functions may render the processed data indistinguishable from the original data. For SignFi and Wiar, the optimal cases apply 41 and 71 basis functions, respectively. SignFi requires fewer functions than Wiar since the environment and human body are more static during the GR task, with only hand movements affecting Wi-Fi signals. This may reduce the complexity of the CSI data and domains for GR. As a result, fewer basis functions can effectively extract features and reduce measurement errors.

D. Evaluation on FSL

One of the key motivations for employing FSL to mitigate the domain shift problem is avoiding extensive new domain data collection, which can be costly for Wi-Fi sensing tasks. Therefore, the number of shots K in the support set is an

important hyperparameter. As depicted in Fig. 6, when the number of query samples keep same, target domain performance improves as K increases. Especially for SignFi, the target domain accuracy can achieve approximately 100% when K equals 9. This is because more target domain information is provided to the model as K increases. However, larger K requires more target domain data, potentially restricting real-world deployment. While more shots boost performance, the selection of K must balance accuracy gains against data requirements for feasible implementation.

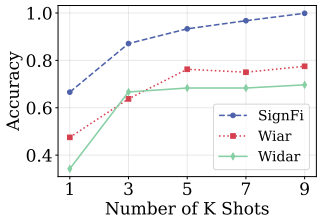

Fig. 6: Classificatio accuracy varies with the number of K support samples.

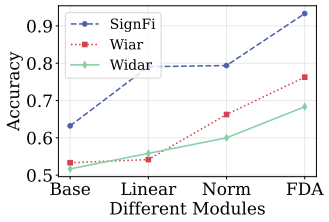

Fig. 7: The effect of linear probe, L_2 norm, and FDA in our proposed method.

E. Ablation Study

In this section, we analyze the impact of different techniques in our method. As Fig. 7 shows, all techniques improve sensing accuracy. For our customized PTN, we examine the linear probe and L_2 norm. The linear probe substantially boosts SignFi's performance, likely due to a large number of categories in SignFi, where the additional linear layer facilitates feature extraction. The L_2 norm also provides gains by enabling more accurate embedding similarity comparisons. Among these techniques, FDA preprocessing increases the accuracy most. This suggests that the FDA-processed CSI tensor contains more valuable data that can be better analyzed.

V. Conclusions

In this paper, we proposed an FDA-assisted FSL method to mitigate the domain shift issues in Wi-Fi sensing with only a few labeled data. To remove measurement errors and uncover key characteristics of the sensing data, we applied FDA with Fourier bases to preprocess the input CSI tensors. Then, a customized PTN is designed to extract discriminative features and improve classification performance on unseen domains. We extensively evaluated the effectiveness of our method across different tasks and datasets. Our results demonstrated that our approach can mitigate domain shift problems effectively.

Acknowledgments

This work is supported in part by the NSF (CNS-2321763, CNS-2319343, CNS-2317190, IIS-2306791, IIS-2306789, CNS-2319342, and CNS-2107190).

References

[1] Y. Ma, G. Zhou, and S. Wang, "WiFi sensing with channel state information: A survey," *ACM Computing Surveys (CSUR)*, vol. 52, no. 3, pp. 1–36, 2019.

[2] Y. Ren, S. Tan, L. Zhang, Z. Wang, Z. Wang, and J. Yang, "Liquid level sensing using commodity WiFi in a smart home environment," *Proc. ACM Interact. Mob. Wearable Ubiquitous Technol.*, vol. 4, no. 1, mar 2020.

[3] S. Tan, L. Zhang, and J. Yang, "Sensing fruit ripeness using wireless signals," in *2018 27th international conference on computer communication and networks (ICCCN)*. IEEE, 2018, pp. 1–9.

[4] Y. Ma, G. Zhou, S. Wang, H. Zhao, and W. Jung, "SignFi: Sign language recognition using WiFi," *Proceedings of the ACM on Interactive, Mobile, Wearable and Ubiquitous Technologies*, vol. 2, no. 1, pp. 1–21, 2018.

[5] Y. Wang, J. Liu, Y. Chen, M. Gruteser, J. Yang, and H. Liu, "E-eyes: device-free location-oriented activity identification using fine-grained WiFi signatures," in *Proceedings of the 20th annual international conference on Mobile computing and networking*, 2014, pp. 617–628.

[6] X. Wang, C. Yang, and S. Mao, "TensorBeat: Tensor decomposition for monitoring multiperson breathing beats with commodity WiFi," *ACM Transactions on Intelligent Systems and Technology (TIST)*, vol. 9, no. 1, pp. 1–27, 2017.

[7] X. Wang, L. Gao, S. Mao, and S. Pandey, "CSI-based fingerprinting for indoor localization: A deep learning approach," *IEEE transactions on vehicular technology*, vol. 66, no. 1, pp. 763–776, 2016.

[8] A. Goldsmith, *Wireless communications*. Cambridge university press, 2005.

[9] W. Jiang, C. Miao, F. Ma, S. Yao, Y. Wang, Y. Yuan, H. Xue, C. Song, X. Ma, D. Koutsonikolas *et al.*, "Towards environment independent device free human activity recognition," in *Proceedings of the 24th annual international conference on mobile computing and networking*, 2018, pp. 289–304.

[10] C. Yang, X. Wang, and S. Mao, "TARF: Technology-agnostic RF sensing for human activity recognition," *IEEE journal of biomedical and health informatics*, vol. 27, no. 2, pp. 636–647, 2022.

[11] H. Kang, Q. Zhang, and Q. Huang, "Context-aware wireless-based cross-domain gesture recognition," *IEEE Internet of Things Journal*, vol. 8, no. 17, pp. 13 503–13 515, 2021.

[12] S. Ding, Z. Chen, T. Zheng, and J. Luo, "RF-Net: A unified meta-learning framework for RF-enabled one-shot human activity recognition," in *Proceedings of the 18th Conference on Embedded Networked Sensor Systems*, 2020, pp. 517–530.

[13] R. Xiao, J. Liu, J. Han, and K. Ren, "OneFi: One-shot recognition for unseen gesture via COTS WiFi," in *Proceedings of the 19th ACM Conference on Embedded Networked Sensor Systems*, 2021, pp. 206–219.

[14] G. Yin, J. Zhang, G. Shen, and Y. Chen, "Fewsense, towards a scalable and cross-domain Wi-Fi sensing system using few-shot learning," *IEEE Transactions on Mobile Computing*, 2022.

[15] T. Zhao, X. Wang, and S. Mao, "Cross-domain, scalable, and interpretable rf device fingerprinting," in *Proc. IEEE INFOCOM 2024*, Vancouver, Canada, May 2024, pp. 1–10.

[16] J. O. Ramsay, "When the data are functions," *Psychometrika*, vol. 47, pp. 379–396, 1982.

[17] F. Rossi, N. Delannay, B. Conan-Guez, and M. Verleysen, "Representation of functional data in neural networks," *Neurocomputing*, vol. 64, pp. 183–210, 2005.

[18] J.-L. Wang, J.-M. Chiou, and H.-G. Müller, "Functional data analysis," *Annual Review of Statistics and its application*, vol. 3, pp. 257–295, 2016.

[19] Y. Wang, Q. Yao, J. T. Kwok, and L. M. Ni, "Generalizing from a few examples: A survey on few-shot learning," *ACM computing surveys (csur)*, vol. 53, no. 3, pp. 1–34, 2020.

[20] J. Snell, K. Swersky, and R. Zemel, "Prototypical networks for few-shot learning," *Advances in neural information processing systems*, vol. 30, 2017.

[21] L. Guo, L. Wang, C. Lin, J. Liu, B. Lu, J. Fang, Z. Liu, Z. Shan, J. Yang, and S. Guo, "Wiar: A public dataset for WiFi-based activity recognition," *IEEE Access*, vol. 7, pp. 154 935–154 945, 2019.

[22] Y. Zhang, Y. Zheng, K. Qian, G. Zhang, Y. Liu, C. Wu, and Z. Yang, "Widar3.0: Zero-effort cross-domain gesture recognition with Wi-Fi," *IEEE Transactions on Pattern Analysis and Machine Intelligence*, vol. 44, no. 11, pp. 8671–8688, 2021.